Reduction of Transmitted 2nd Harmonics Using an Adaptive Method by Simulated Annealing

Huynh, Thong[1]; Haugen, Geir[2]; Hoff, Lars[1]

[1]Department of Microsystems, University of South-Eastern Norway, Horten, Norway
[2]GE Vingmed Ultrasound AS, Horten, Norway

This is an Accepted Manuscript of an article published by IEEE Online in *2017 IEEE International Ultrasonics Symposium (IUS)* on November 2, 2017, available online: https://doi.org/10.1109/ULTSYM.2017.8092111

Huynh, T., Haugen, G., & Hoff, L. (2017, September 6-9). Reduction of Transmitted 2nd Harmonics Using an Adaptive Method by Simulated Annealing [Conference presentation]. *2017 IEEE International Ultrasonics Symposium (IUS)*. Washington, DC. https://doi.org/10.1109/ULTSYM.2017.8092111

Reduction of Transmitted 2^{nd} Harmonics Using an Adaptive Method by Simulated Annealing

Thong Huynh[1], Geir Haugen[2] and Lars Hoff[1]
[1]Department of Microsystems, University College of Southeast Norway, Horten, Norway
[2]GE Vingmed Ultrasound AS, Horten, Norway

***Abstract*—Second harmonic imaging relies on the 2^{nd} harmonic of the transmit frequency f_0 generated by the waves propagation in tissue. This method suffers from noise because signal transmitting at the desired receive frequency $2f_0$. Transmitted 2^{nd} harmonic may be originated from both linear, e.g. sidebands in the transmit spectrum, and/or nonlinear effects in the transducer and transmitting electronics. In this paper, an adaptive method, simulated annealing, was utilized to find optimized electrical excitation waveforms to suppress the 2^{nd} harmonic components of the emitted ultrasound pulses. Experimental results on two different kinds of transducer pulsers show that the method can find excitation waveforms which generate sufficient low 2^{nd} harmonic (-30dB of the main lobe) at the output for a successful 2^{nd} harmonic imaging.**

***Index Terms*—second harmonic imaging, optimization, excitation waveforms, simulated annealing**

I. Introduction

Second harmonic imaging is a preferred ultrasound imaging modality, mainly due to its ability to suppress reverberations[1]. The system transmits an ultrasound pulse at center frequency f_0. Nonlinear propagation creates the 2^{nd} harmonic of this frequency in the tissue, and echoes at frequency $2f_0$ are used to construct the image. This technique requires good control of the transmit frequency, to prevent components at $2f_0$ from being transmitted by the transducer and interfering with the 2^{nd} harmonic created in the tissue.

One method to suppress the transmitted 2^{nd} harmonic called alternate phasing was introduced by Krishnan et al. [2]. Only simulation results were presented, and this method causes grating lobes which may introduce artifacts into the image. Another method is designing an optimized excitation waveform for the transmit system to compensate for the nonlinearity of the system. This method has been applied to capacitive micro-machined ultrasonic transducers (cMUTs) [3]. The compensation can be designed from knowledge of the nonlinear properties of the transmit system. However, an accurate mathematical description of the nonlinear system is often difficult to achieve, especially since the detailed internal structure can be difficult to access and model correctly. Alternatively, a more empirical adaptive method can be applied, by measuring the input to output relationship. This paper presents such an approach to minimize the transmitted 2^{nd} harmonic from a clinical ultrasound scanner. Simulated annealing was selected as the optimization algorithm, and used to find the optimal excitation waveform $\hat{\mathbf{u}}$ that minimizes a cost function C calculated from the emitted 2^{nd} harmonic energy,

$$\hat{\mathbf{u}} = \underset{\mathbf{u}}{argmin}(C(\mathbf{u}))\,, \tag{1}$$

where $\mathbf{u} = [u(0), u(1), ..., u(L)]$ is the waveform definition vector, and L the total number of samples in the transmit waveform. The cost function C is calculated from measured transmitted ultrasound pulses, and mainly designed to depress the transmitted 2^{nd} harmonic while confining high energy in the fundamental. The freedom to define the excitation waveforms $\mathbf{u}$ is limited by the capabilities of the actual driving electronics. In this study, 2 different pulsers were studied: One 3-level pulser with generating frequency f_{gen} 200 MHz, and one 31-level generator with f_{gen} 50 MHz, respectively.

II. Method

A. Simulated Annealing

Simulated annealing (SA) is an optimization algorithm designed to find a sufficiently good solution where the solution space is huge. It was considered appropriate for the optimization problem in this study, as there are m^L possibilities for an m-level waveform of L samples. The algorithm imitates the annealing process used in metallurgic [4], and is controlled by the acceptable rate and current temperate as its state [5]. In general, the SA algorithm requires two functions for a particular problem: the neighbor function determining how the inputs are perturbed, and the cost function evaluates the quality of a solution based on defined criteria.

1) The neighbor function:

a) 3-level waveform: The 3-level waveform is modified by changing the widths of the positive and negative pulses. Two vectors are used to define the shape of the 3-level waveform, as illustrated in Fig. 1. The first vector $\mathbf{s} = [s_1, s_2, ..., s_n]$ stores the switching positions of the pulse as sample indices. Notice that $s_{i-1} \leqslant s_i \leqslant s_{i+1} \leqslant L$ where L is the number of samples of the pulse. The second vector $\mathbf{l} = [l_1, l_2, ..., l_n]$ decides the level for each pulse segments, $l_i \in \{-1, 0, 1\}$. The combination of the two vectors $\mathbf{s}$ and $\mathbf{l}$ defines a solution in the SA algorithm. To reduce complexity, the length of the pulse L, the number of switchings n, and the level vector $\mathbf{l}$ were all fixed. The neighbor function generates a new waveform by randomly changing the pulse widths $\mathbf{s}$ of the current waveform,

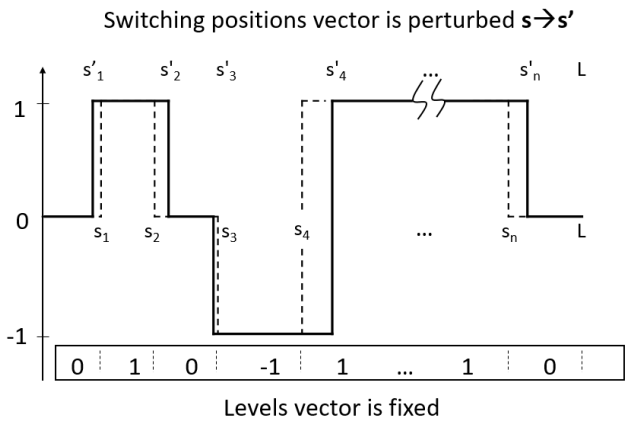

Fig. 1. Perturbation mechanism for the 3-level waveform. The new pulse (solid line) is generated from the current pulse (dashed line) by changing the switching times in the vector **s**.

with the difference from old to new pulse width limited by a predefined maximum $\Delta s_{max} > 0$

$$\mathbf{s}' = \mathbf{s} + \Delta\mathbf{s}\,, \tag{2}$$

where $\Delta\mathbf{s}$ are random integers, $-\Delta s_{max} \leqslant \Delta s_i \leqslant \Delta s_{max}$. This modification scheme creates a new waveform as a slightly modified version of the current waveform, a *neighbor*, as required in the algorithm.

b) 31-level waveform: The 31-level pulser has a DAC output stage that can set the output level to any integer value from -15 to $+15$. The output levels at discrete time positions are determined by a vector $\mathbf{s} = [s_1, s_2, ..., s_L]$, where L is the number of samples. Notice that the vector **s** in this case entirely differs from the case of 3-level waveform, which identifies the switching positions. Frequency components outside the transducer bandwidth will not contribute to the acoustic pulse, but dissipate as heat in the transducer. To reduce this, a digital low-pass filter was applied to the waveform **s**, and this filtered pulse was scaled to the maximum level ± 15. The resulting pulse **u** was then sent to the pulser.

Fig. 2 illustrates the perturbation method for the 31-level waveform, used in the SA algorithm. As in the previous case, the pulse length L was fixed. The LPF is a Chebyshev low-pass filter with cutoff frequency 5 MHz, equal to the upper frequency bound of the transducer. Based on the original trial waveform **s**, the neighbor function generates a new candidate waveform $\mathbf{u}'$ by first perturbing **s** to $\mathbf{s}'$ as described above in (2), then filtering and scaling it.

2) The cost function: The quality of the transmitting acoustic pulses is described by a cost function, quantifying how much the actual pulse suitable for 2^{nd} harmonic imaging. The cost function is defined in the frequency domain, based on the power spectrum of the measured acoustic pulse $\mathbf{y}_i$ resulting from a pulse definition $\mathbf{u}_i$. Notice that the 2^{nd} harmonic level is not at a specific discrete spectral component but a band of frequencies. The cost function definition associates a weight to every discrete spectral component. Positive weights signify

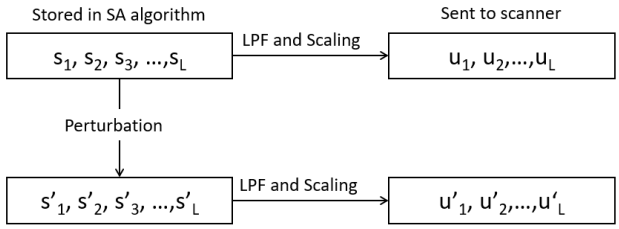

Fig. 2. Perturbation mechanism for the 31-level waveform. The current output waveform **s** is perturbed to the new neighbor waveform $\mathbf{s}' = \mathbf{s} + \Delta\mathbf{s}$. These waveforms are low-pass filtered and scaled to **u** or $\mathbf{u}'$, then sent to the DAC driving the transmit electronics.

a high cost, i.e. a negative property that should be avoided, while negative cost function values are considered beneficial.

The weighting curve for the cost function is illustrated in Fig. 3. High positive weights are assigned to frequency components in the range of the 2^{nd} harmonic of the transmit frequency, as these shall be suppressed. In the transmit band ($f_0 = 1.67\ MHz$), the weights are negative, as this is where we want the transmit energy confined. Outside these ranges, below the transmit band and above the 2^{nd} harmonic, a lower positive weight is assigned. These frequencies do not contribute to the transmit pulse but dissipate as heat in the transducer, and need to be suppressed, but at a lower priority than frequencies around the 2^{nd} harmonic.

The cost function is calculated from the measured ultrasound pulse **y** as

$$C(\mathbf{u}) = \sum_{f=0}^{f_s/2} w(f) * PSD(f, \mathbf{y}) \tag{3}$$

where $f_s = 100MHz$ is the sampling frequency of the recorded signal, and $PSD(f, \mathbf{y})$ the power spectrum density of the ultrasound pulse **y**.

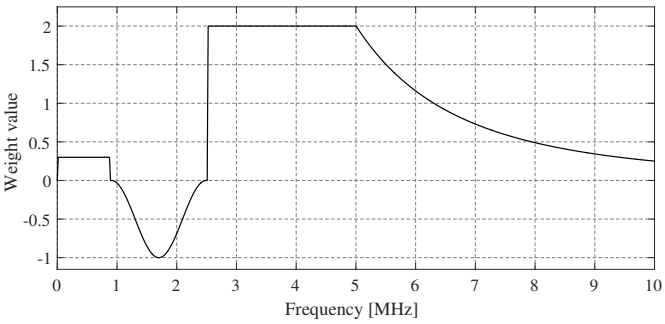

Fig. 3. Weight curve $w(f)$ for the cost function. Positive values are associated with a high cost and should be suppressed, while negative values are considered beneficial.

B. Experimental setup

Transmitted ultrasound pulses from an ultrasound scanner were measured in a water tank using a hydrophone (HGL0200, ONDA Corp., Sunnyvale, CA). The pulses were measured

close to the transducer surface, at distance 3 mm, before harmonics from nonlinear propagation had developed. The hydrophone aperture is $200\mu m$, and the hydrophone was calibrated from 1 to 20 MHz in magnitude. Phase calibration for the hydrophone was estimated from the provided magnitude values, using the Kramers-Kronig relation. A preamplifier with gain 20 dB (AG-2010, Onda), designed to match the hydrophone, was connected to the hydrophone. Its output was digitized by an oscilloscope (PicoScope 5244A, PicoTech, St Neots, UK) and sent to a computer via USB . The Simulated Annealing algorithm was implemented in MATLAB (The Mathworks, Natick, MA, USA). The cost function was calculated from the recorded pulse $\mathbf{y}$, and this was used to modify the pulse definition, from $\mathbf{u}$ to $\mathbf{u}'$. The modified pulse definition $\mathbf{u}'$ was then sent to the ultrasound scanner through an network communication via Ethernet. The scanner used this new waveform to generate and transmit a new output pulse $\mathbf{y}'$, which was again measured with the hydrophone, and this procedure was repeated for a preset number of iterations. The method was applied to optimize both types of probes, one using a 3-level pulser, the other using a 31-level pulser.

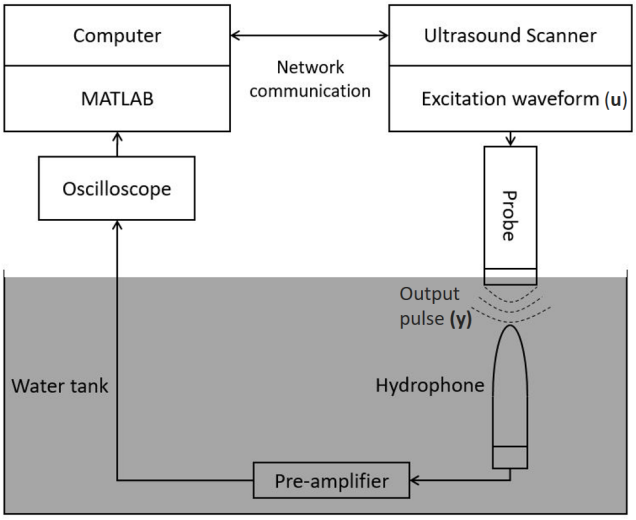

Fig. 4. The acoustic measurement system. An excitation waveform **u** was defined in the ultrasound scanner to drive the probe. The resulting ultrasound pulse **y** was measured by the hydrophone, digitized, and analyzed using Matlab, by calculating a the cost function $C(\mathbf{u})$. From this, a new waveform **u'** was defined using the SA algorithm. It was again transferred to the ultrasound scanner via Ethernet connection, to generate the new output pulse **y'**. This process repeated a preset number of iterations.

III. Results

The scanner was configured to transmit at full mechanical index MI=1.3, assumed to maximize the harmonic distortion in the transmit stage. The cooling scheme for the SA algorithm was $T_n = \alpha^n T_0$ with $\alpha = 0.95$, and the optimization procedure was run for 20 000 iterations. The initial acceptance rate was chosen relative low (40%), and a quick cooling schedule was used to avoid the solution waveform entering inefficient shapes that are not allowed by ultrasound scanner. For the 3-level waveform, the waveform length was fixed to $1.2\mu s$, corresponding to 2 periods of the fundamental frequency 1.67 MHz, or $L = 240$ samples. The number of switchings was fixed to $n = 12$ and the level vector $\mathbf{l}$ to $\mathbf{l} = [1, 0, 1, 0, -1, 0, 1, 0, -1, 0, -1, 0]$. For the 31-level waveform, the length was fixed to $1.8\mu s$, 1 cycle longer than the 3-level waveform, to get a better result because the 31-level probe showed a stronger nonlinearity in our test.

The optimized waveforms for the 3-level and 31-level pulser are presented in Fig. 5 and Fig. 6 respectively. As an illustration, these results are compared with 2 typical excitations with the same length: a 2-cycle square wave for the 3-level and a Gaussian-modulated sinusoidal wave for the 31-level waveform. Using the excitations found by this method, the measured transmitted 2^{nd} harmonic are 40dB and 30dB lower than the fundamental for the 3-level and 31-level pulser respectively, and about 15dB better than 2 typical excitations at the 2^{nd} harmonic .

IV. Discussion

To limit the optimization time, the degrees of freedom of the input waveforms were limited. Better results might have been achieved if these constraints had been relaxed and the waveforms allowed to change more freely. This would have increased the solution space, but also convergence time. Efficient convergence is critical in this study, since real ultrasound pulses have to be generated, transmitted and measured for each iteration. This requires a good initial guess and limiting the solution space to a promising sub-space. This is the reason for limiting the number of switchings in the 3-level waveform to what might look like a low number, as many switchings will increase energy at the high frequencies, dissipating as heat in the transducer, while not reducing the emitted 2^{nd} harmonic.

Both in Fig. 5b and Fig. 6b, the optimized excitation waveforms contain more energy at the 2^{nd} harmonic band than the reference waveforms do, while the resulting ultrasound output pulses contain less 2^{nd} harmonic, see Fig. 5d and Fig. 6d). This illustrates how the optimization process works on the measured ultrasound pulses: The transmitted 2^{nd} harmonic is reduced by adding some 2^{nd} harmonic at a different phase to the input pulses, counteracting non-ideal effects in the whole system, e.g. quantization errors and nonlinearity in the electronic and transducer.

Simulated annealing was chosen as the optimization algorithm in this study, but other optimization algorithms might also be tested, potentially improving the results by faster convergence or finding more optimal waveforms. The optimization method can be also adapted to meet other criteria than reduction 2^{nd} harmonics, by defining a different cost function based on these criteria.

V. Conclusion

The described method was tested on 2 typical types of pulser used in clinical ultrasound scanners, and it can find optimized excitation waveforms suppressing the transmitted 2^{nd} harmonic level to 30 dB below the main lobe in both cases. This method is particularly suited to compensate for

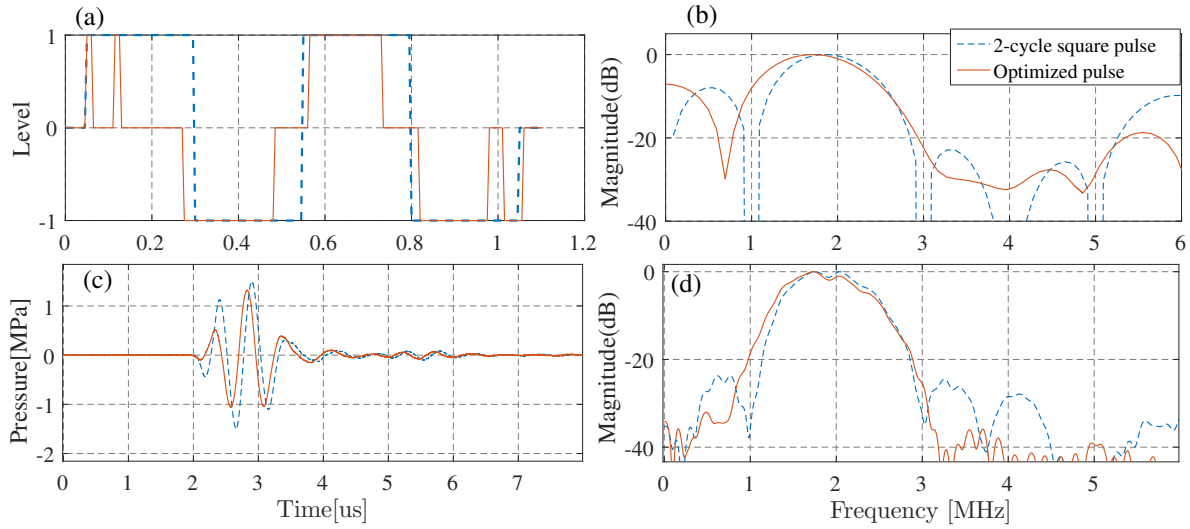

Fig. 5. Optimization results for the 3-level pulser. The optimized waveform (red) is compared with the 2 cycles square wave at the fundamental frequency 1.67 MHz (blue-dashed). The upper graphs show the pulse definitions (*a*) and their power spectra (*b*), while the lower graphs show the measured acoustic pulses (*c*) and their power spectra (*d*).

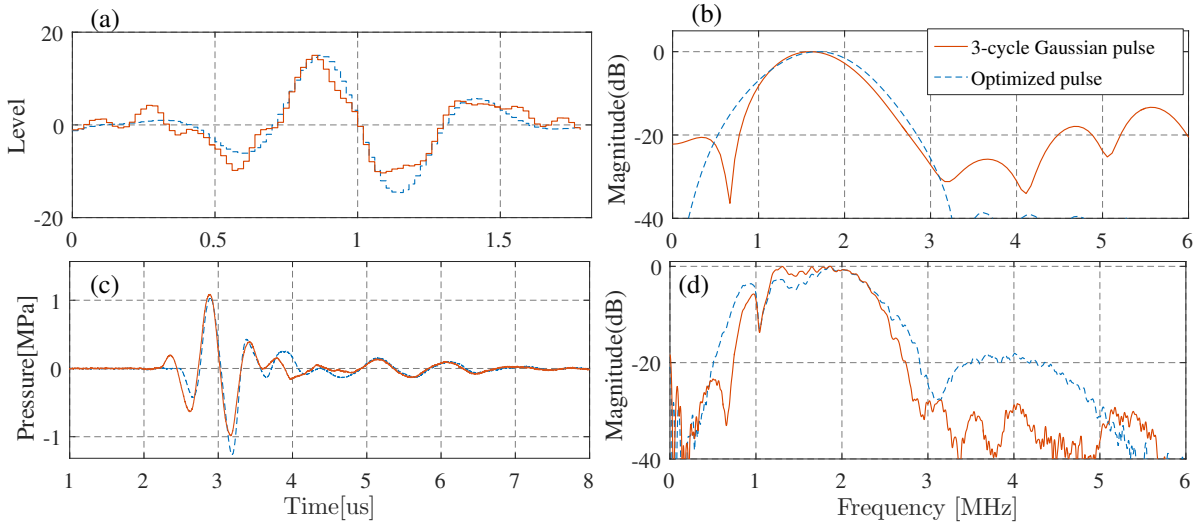

Fig. 6. Optimization results for the 31-level pulser. The optimized waveform (red) is compared with the 3 cycles sinusoidal wave at the fundamental frequency 1.67 MHz enclosed in a Gaussian envelope (blue-dashed). The upper graphs show the pulse definitions (*a*) and their power spectra (*b*), while the lower graphs show the measured acoustic pulses (*c*) and their power spectra (*d*).

nonlinear effects in the probes and transmit electronics, i.e. to compensate for phenomena not fully described by a linear impulse response. The authors would like to point out that the results presented here are on an experimental system, and have no relation to the released scanner and its performance.

REFERENCES

[1] M. Averkiou, "Tissue harmonic imaging," in *2000 IEEE Ultrasonics Symposium*, vol. 2, Oct. 2000, pp. 1563–1572 vol.2.

[2] S. Krishnan, J. D. Hamilton, and M. O'Donnell, "Suppression of propagating second harmonic in ultrasound contrast imaging," *IEEE Transactions on Ultrasonics, Ferroelectrics, and Frequency Control*, vol. 45, no. 3, pp. 704–711, May 1998.

[3] S. Zhou, P. Reynolds, and J. Hossack, "Precompensated excitation waveforms to suppress harmonic generation in MEMS electrostatic transducers," *IEEE Transactions on Ultrasonics, Ferroelectrics, and Frequency Control*, vol. 51, no. 11, pp. 1564–1574, Nov. 2004.

[4] S. Brooks and B. Morgan, "Optimization using simulated annealing," *Statistician*, vol. 44, no. 2, pp. 241–257, 1995.

[5] S. Ledesma, G. Avia, and R. Sanchez, "Practical considerations for simulated annealing implementation," in *Simulated Annealing*, C. Ming, Ed. InTech, Sep. 2008.